VANISHING POINT DETECTION FOR ARCHITECTURAL PHOTOGRAMMETRY

Frank A. van den Heuvel
Faculty of Civil Engineering and Geosciences
Delft University of Technology
Thijsseweg 11, 2629JA Delft, The Netherlands
E-mail: F.A.vandenHeuvel@geo.tudelft.nl

Commission V, Working Group 5

KEY WORDS: vanishing point, image analysis, geometric constraints, adjustment, architecture

ABSTRACT

A priori object information like parallelism and perpendicularity can be very useful for 3D-reconstruction, especially in architectural photogrammetry. With digital close-range imagery parallelism of object lines can be exploited by applying automatic vanishing point detection. This image analysis technique allows the detection of parallel object lines and leads to their spatial orientation in the camera system. The latter can be used for 3D-reconstruction as well as for the determination of the exterior orientation parameters of the image involved. A priori object information in the form of angles between object lines (like perpendicularity) can improve vanishing point detection considerably.

The paper gives a short overview of research in vanishing point detection that has a long history in the computer vision community. A new method for vanishing point detection that is based on rigorous statistical testing and perpendicularity constraints is presented. First results of the application of this method to imagery of buildings are discussed.

1. INTRODUCTION

Lines in an image that are projections of parallel lines in object space intersect in one point in the image plane, the so-called vanishing point. This holds under the assumption of a perfect pin-hole camera model. The vanishing point is found as the intersection of the interpretation planes associated with the image lines and the image plane (figure 1). In case of parallelism of image plane and object lines the vanishing point is at infinity. To avoid this singularity, the vanishing point can be defined as the intersection of the interpretation planes and the Gaussian sphere (Shufelt, 1996). In other words: the vanishing point is related to an orientation in object space represented by a point on the Gaussian sphere. In the sequel the contradictory term "vanishing point orientation" is used to denote this spatial orientation.

With the detection of a vanishing point the orientation of the object lines is known in the camera system. With the detection of several vanishing points the resulting orientations can be used for object reconstruction and for exterior orientation (van den Heuvel, 1997). In all applications where parallel object lines are present, vanishing point detection can be a valuable tool for the automation of these major tasks of vision systems.

Vanishing point detection is traditionally applied for the navigation of autonomous vehicles or robots in indoor or outdoor man-made environments (Pla et al.,1997; Straforini et al., 1992). This paper concentrates on the application of vanishing point detection to terrestrial close-range imagery of buildings. An example of this application can be found in (Collins, 1993). An application to building reconstruction from aerial imagery is investigated in (Shufelt, 1996). The main difference between applications for navigation and for object reconstruction is the fact that navigation applications demand fast algorithms because of their real-time nature. In applications for object reconstruction this limiting condition can be dropped, as full automation is generally not possible and thus operator interaction will be the bottleneck for the processing time.
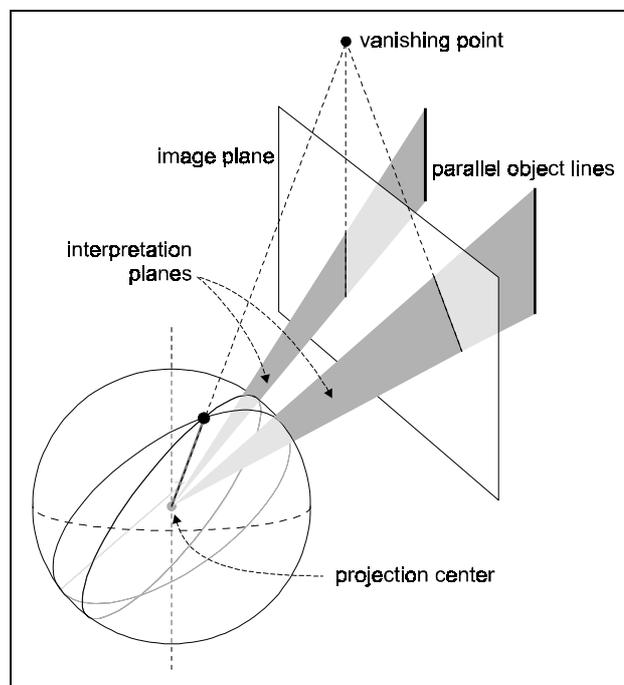

Figure 1: Vanishing point on image plane and Gaussian sphere after (Shufelt, 1996)

After a discussion of the characteristics of existing vanishing point detection techniques in section 2, a new

technique is presented in section 3. This technique is more computationally expensive than existing techniques, but it is rigorous from a statistical point of view. In section 4 some examples of applications of the proposed technique are presented.

2. VANISHING POINT DETECTION TECHNIQUES

Straight line features have to be extracted from the image prior to the vanishing point detection. This preprocessing step will not be discussed here as it has been thoroughly investigated (Burns et al., 1986; Förstner, 1988). In this section only the major characteristics of previous research in vanishing point detection are emphasized.

Vanishing point detection can be regarded as the search for a set of lines that intersect at one point in the image plane. It is assumed that the largest sets of lines correspond to vanishing points. As a vanishing point can be outside the image boundaries and even at infinity, the search area is unbounded. In order to bound the search domain, most vanishing point detection techniques apply a specific representation of the image lines.

In Straforini (1993) a representation in a bounded and partitioned polar space is used. Each line is represented by a point in polar space and grouped with lines that are located in the same partition. In this approach there are restrictions to the relative position of camera and object. Other shortcomings are the dependency of the partitioning of the polar space on the orientation of the camera relative to the object and the fact that the precision of the line parameters is not taken into account.

Most of the vanishing point detection techniques use a Hough transform approach in which the parameter space is located on a so-called Gaussian sphere, see for instance (Lutton et al., 1994). In these approaches interpretation planes associated with image lines are intersected with a (unit) sphere with its center positioned at the projection center. Then these intersections are great circles and vanishing points are found as intersections of great circles (figure 1). In order to detect a vanishing point a quantization of the sphere is performed and the number of great circles running through each bucket (or pixel) of the grid on the sphere is counted. Then maxima are detected and assumed to correspond to vanishing points. In this approach there are no restrictions on the orientation of the camera and the search space is limited. A disadvantage is the choice for the quantization of the sphere to be made.

In Shufelt (1996) several alternatives for Gaussian sphere-based vanishing point detection are investigated, including two complementary methods. The first method integrates a priori knowledge on camera orientation and knowledge on the geometry of the imaged objects. The second method applies edge error modeling in order to account for the precision (and length) of the lines. These and existing methods are combined resulting in 24 experimental options that are tested on aerial imagery.

In the next section a new method for vanishing point detection is presented that applies geometric object information, but does not use the Hough transform and thereby eliminates its disadvantages. This method is tested on close-range imagery of buildings.

3. A NEW METHOD FOR VANISHING POINT DETECTION

The principal goal of the new method for vanishing point detection is the robust detection of image lines that intersect at the three main vanishing points, under the assumption of perpendicularity between the three corresponding orientations in object space. The image line feature extraction is not part of the procedure but considered as a preprocessing step. The principles of the method can be used for the detection of an arbitrary number of vanishing points with or without a priori information on object geometry.

3.1 Overview

The method proposed here is based on the statistical testing of the intersection hypotheses of combinations of 3 image lines or rather the intersection of the 3 interpretation planes associated with these lines. This test is discussed in the next section. The major steps of the procedure are the following (the procedure is discussed in detail in section 3.3):

- compute statistical test values of all combinations of 3 interpretation planes (i.e. image lines)
- detection of groups of lines that intersect in a vanishing point by clustering based on these test values (section 3.4)
- for the largest clusters: statistical testing of line error hypotheses using all condition equations and iterative elimination of rejected lines
- final selection of largest cluster as the vanishing point cluster
- restart of the procedure for the next vanishing point with the use of information on perpendicularity to previously detected vanishing point(s)
- after detection of the 3 vanishing points: statistical testing of all condition equations (for intersection and perpendicularity)

3.2 The statistical test of the intersection constraint

The intersection constraint introduced in the previous section is formulated with the normals to the interpretation planes of the 3 lines involved. The image lines are represented by the image coordinates of the end points (figure 2). The image coordinates are assumed to be corrected for lens and image plane distortions. Then a point in the image corresponds to a direction in object space (in the coordinate system of the camera):

$$\mathbf{x} = (x, y, -c), \quad c: \text{camera constant} \qquad (1)$$

The normal to the interpretation plane of the image line *i* with end points a and b is found with:

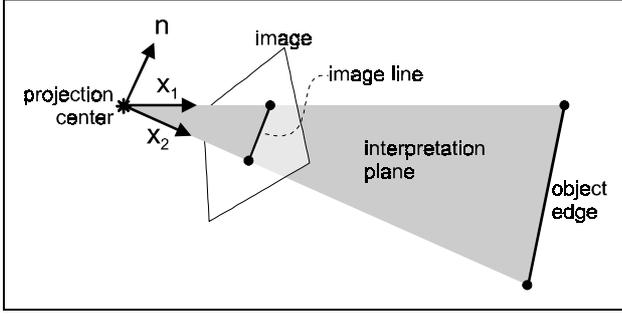$$\mathbf{n}^i = \mathbf{x}^a \times \mathbf{x}^b \qquad (2)$$

Figure 2: The interpretation plane

The intersection constraint can be written as the determinant of the matrix build from the 3 normal vectors *i*, *j* and *k* (van den Heuvel and Vosselman, 1997):

$$\left[\mathbf{n}^i, \mathbf{n}^j, \mathbf{n}^k\right] = \det(\mathbf{n}^i, \mathbf{n}^j, \mathbf{n}^k) = 0 \qquad (3)$$

In case the lines do not (perfectly) intersect this constraint will result in a misclosure (*m*):

$$\left[\mathbf{n}^i, \mathbf{n}^j, \mathbf{n}^k\right] = m \qquad (4)$$

The hypothesis of interpretation plane intersection is tested with the normalised misclosure relative to a critical value (*cv*):

$$\left[\mathbf{n}^i, \mathbf{n}^j, \mathbf{n}^k\right] = n \qquad (5)$$

The standard deviation of the misclosure (σ_m) is computed from the covariance matrix of the image coordinates (σ_m):

$$\left[\mathbf{n}^i, \mathbf{n}^j, \mathbf{n}^k\right] = \det(\mathbf{n}^i, \mathbf{n}^j, \mathbf{n}^k) = C \qquad (6)$$

with **b** the vector of partial derivatives. The part of **b** for image point *a* can be written as:

$$\mathbf{b}^a = \frac{\partial m}{\partial \mathbf{n}^i} \frac{\partial \mathbf{n}^i}{\partial \mathbf{x}^a} \qquad (7)$$

The camera constant is assumed to be error free. For the image points covariance matrix several options are available for the stochastic model:

- If lines are extracted using an edge detection approach, the variances of the coordinates of the end points are assumed to decrease linearly with the length of the line in pixels.
- For lines that are extracted manually by measurement of their end points, a constant variance is assumed for all end point coordinates.

Precision information available from the feature extraction procedure could be used for the stochastic model, but then the model does not account for imperfections of the camera model or for possible deformations of the object. Line orientation does not play a role in the stochastic model as only precision information perpendicular to the line affects the precision of the interpretation plane normals.

3.3 The procedure

In this section the procedure for vanishing point detection is discussed in detail. Although the method consists of

the steps in section 3.1 there are differences between the parts of the procedure for each vanishing point. The differences relate to the use of perpendicularity assumptions.

3.3.1 The first vanishing point

The intersection constraint introduced in section 3.2 involves 3 lines. If a statistical test is computed for each combination of 3 lines, we have to deal with an $O(n^3)$ problem (*n* is the number of image lines). Although computing efficiency is not a design goal, the order is reduced to n^2 by selecting a line of the first vanishing point, the so-called start-line. The longest line is chosen as the start-line and in many cases this line belongs to one of the 3 vanishing points to be detected. If this is not the case the start-line can be chosen manually. The procedure for the first vanishing point runs as follows:

- The test value of (*n*-1)(*n*-2)/2 combinations of the start-line and two other image lines is computed according to (5).
- Lines are clustered using the results of the testing (section 3.4).
- For the largest clusters an adjustment is set up, based on all (independent) constraints in the cluster and a line error hypothesis is tested for each line.
- Rejected lines are removed from the cluster and the adjustment is repeated until all lines are accepted.
- The largest cluster is selected as the vanishing point cluster.

From the adjustment the adjusted 3D orientation of the first vanishing point results. This orientation is input to the detection procedure of the next vanishing point.

3.3.2 The second vanishing point

Because the orientation of the second vanishing point is assumed to be perpendicular to the orientation of the first, the normal to the interpretation plane of the start-line can be replaced by the orientation of the first vanishing point ($\mathbf{v}_1$) in the procedure for the first vanishing point. $\mathbf{v}_1$ results from the normals of two interpretation planes *i* and *j* of the first vanishing point:

$$\mathbf{v}_1 = \mathbf{n}_1^i \times \mathbf{n}_1^j \qquad (8)$$

The normals are computed with adjusted observations from (2). The constraint (3) is rewritten as:

$$\left[\mathbf{n}^i, \mathbf{n}^j, \mathbf{v}_1\right] = 0 \qquad (9)$$

Again the computation of the statistical test values is of order n^2. The perpendicularity between the second and third vanishing point orientation is used to detect both vanishing points in one go. Therefore a second statistical test is introduced to test the hypothesis of perpendicularity of the two vanishing points of lines *i* and *j*. The related constraint is:

$$\left(\mathbf{n}^i \times \mathbf{v}_1\right) \cdot \left(\mathbf{n}^j \times \mathbf{v}_1\right) = 0 \qquad (10)$$

Now two sets of test values are available for the clustering. First the clustering is performed using the smallest of the two values. This results in a (largest) combination cluster of lines of the second and third

vanishing point. Then the clustering is repeated using only the lines of the combination cluster and test values from the parallelism test (5). In this way the second vanishing point is detected as a subset of the combination cluster, thereby increasing the chances of a correct detection.

3.3.3 The third vanishing point

For the detection of the third vanishing point the remaining lines of the combination cluster could be used. But in order to use the information contained in the detection of the second (and first) vanishing point, all lines are used for an intersection test that is based on the orientations of the first two vanishing points computed from (8). Now (9) is rewritten as:

$$\left[\mathbf{n}^i, \mathbf{v}_2, \mathbf{v}_1\right] = 0 \qquad (11)$$

The computation of the statistical test values reduces to order n because in fact the third vanishing point is already known with the detection of the first two. This is due to the perpendicularity assumption:

$$\mathbf{v}_3 = \mathbf{v}_1 \times \mathbf{v}_2 \qquad (12)$$

By allowing all lines to be candidate for the detection of each vanishing point – even lines that are in a cluster of a previously detected vanishing point – the lines can be detected that are on (or close to) a so-called horizon line, the line that connects two vanishing points in the image plane (Williamson and Brill, 1989). It is important to detect these lines because an ambiguity in their spatial orientation remains.

3.4 Clustering

The acceptance of statistical test (5) is evidence for the intersection of 3 lines in a point in the image plane. A clustering is applied to the test results that aims at the detection of groups of lines that intersect in one image point. The clustering procedure for the first two vanishing points includes the following steps:
- For each accepted test it is checked whether one of the two lines is present in an existing cluster (the third line is the so-called start-line or a vanishing point orientation). If this is not the case, a new cluster is established.
- If a line of an accepted test is present in an existing cluster, the other line becomes a candidate for the cluster.
- The candidate line becomes a member of the cluster if all the tests of lines already in the cluster and the candidate line are accepted. If this is not the case, a new cluster is established.

This procedure is repeated as long as new clusters are created. In the last iteration all tests are evaluated in the presence of all clusters. The result is that lines can appear in more than one cluster and overlap between clusters can be close to 100%. The major advantage is the reduced sensitivity of the clustering result to the order in which the lines are processed. The largest clusters are analysed in more detail in order to decide which lines

belong to the vanishing point (see the next section). The size of a cluster is defined by the number of lines it contains, or optionally by the sum of the lengths of all lines in the cluster. In the latter case clusters with longer lines are preferred.

In the clustering procedure two critical values are used for evaluation of the statistical tests. One critical value for the candidate test (first step of the procedure) and another value for the membership test (last step of the procedure). Because type I errors (rejection of the intersection hypothesis although it is true) have to be avoided in the clustering phase, for the level of significance (α) the value 0.1% is chosen for the candidate test. For the membership test a lower value for the level of significance is chosen (e.g. 0.01%) in order to avoid the creation of many overlapping clusters.

For the detection of the third vanishing point the clustering procedure can be simplified due to the perpendicularity to the orientations of the first two vanishing points detected previously. For the third vanishing point only one cluster is built from all lines for which the statistical test (5) is accepted.

3.5 Adjustment and testing

The clustering procedure described in the previous section results in groups of lines that are candidates for a vanishing point. For a preset number (e.g. 3) of the largest clusters an adjustment is set up. The functional model contains a complete set of n-2 independent condition equations (n is the number of image lines). These equations have the form of (3), (9) or (11) for respectively the first, second and third vanishing point. After linearisation this model can be written as:

$$\mathbf{B}^T E\{\mathbf{y}\} = \mathbf{0} \ ; \ \mathbf{Q_y} \qquad (13)$$

with:
$E\{\}$	mathematical expectation
$\mathbf{y}$	vector of observations (image coordinates)
$\mathbf{B}$	design matrix (partial derivatives, see (7))
$\mathbf{Q_y}$	covariance matrix of the observations

The solution to this model is presented in (van den Heuvel and Vosselman, 1997).

Two different types of statistical tests are applied. First an overall test or Fisher test is applied by computing the estimated variance of unit weight:

$$(\hat{\sigma}^2 =) \ \frac{\mathbf{m}^T (\mathbf{B}^T \mathbf{Q_y} \mathbf{B})^{-1} \mathbf{m}}{(n-2)} \ < \ cv \, \sigma_0^2 \quad (14)$$

The vector of misclosures ($\mathbf{m}$) is computed from the non-linearised condition equations. The critical value (cv) of this test is derived from the Fisher distribution (degrees of freedom n-2, ∞; α=1%) multiplied with a factor 2 in order to avoid type I errors in this stage of the procedure.
The second test is a line error test, examining the alternative hypothesis of an error in a single line. This is a so-called non-conventional alternative hypothesis (Baarda, 1968) and will not be discussed in detail here. The level of significance for this test is chosen in the

same way as for the overall test. If a line test is rejected, the line is removed from the cluster and the model is built again. This iterative testing procedure stops if all line tests are accepted. The largest cluster of which the overall test and all line tests are accepted is assumed to be the cluster with the lines intersecting at the vanishing point.

After the detection of the three vanishing points a final adjustment is performed. Then the three sets of condition equations used for each vanishing point are combined in one adjustment with the three perpendicularity conditions of the form:

$$(\mathbf{n}_1^i \times \mathbf{n}_1^j) \cdot (\mathbf{n}_2^i \times \mathbf{n}_2^j) = 0 \qquad (\ 15 \ )$$

This is the condition equation for perpendicularity between the orientations of the first two vanishing points (1 and 2), derived from the normals of two interpretation planes (*i* and *j* for each vanishing point). As an option, the inclusion of the perpendicularity constraints can be dependent on the outcome of the statistical test of the perpendicularity hypothesis.

For the final adjustment only lines that are uniquely clustered to one of the vanishing points are used, so horizon lines are excluded. The level of significance for the overall test and line error tests is set to 1%.

Figure 3: Delft image: lines of first, second and third vanishing point (from left to right)
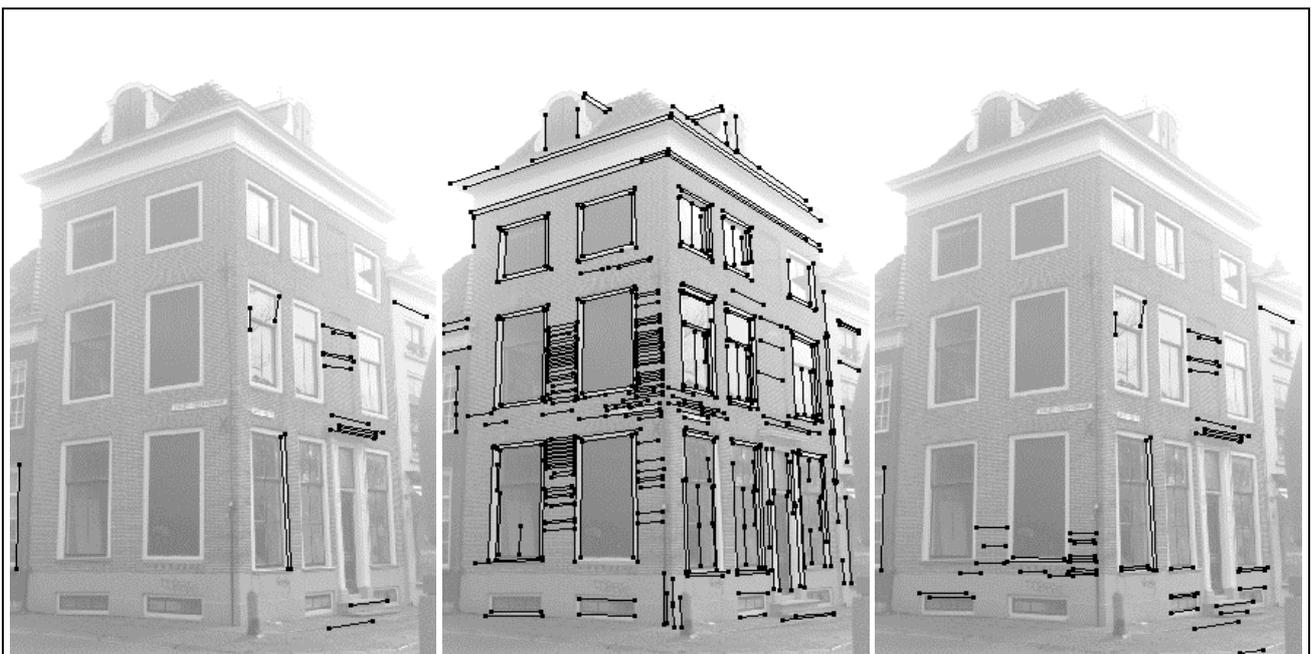

Figure 4: Delft image: rest of the lines, adjusted lines and non-adjusted lines (from left to right)

4. EXAMPLES

In this section two applications of the new method for vanishing point detection are discussed. Both images are taken with a calibrated Kodak DCS420 digital camera with a 20mm lens. The CCD sensor of this camera contains approximately 1500x1000 pixels with a pixel spacing of 9μm. The images are taken from about 1.5m above the ground and as a result they contain a horizon line (the connecting line between the two vanishing points of the horizontal lines, see section 3.3). Before the extraction of straight lines, the images are corrected for lens distortion. Without correction long lines tend to break up in smaller parts due to line curvature. Straight lines were extracted using a line growing algorithm (Förstner, 1988).

4.1 Example 1: image of a historic building

The first image is taken in the historic center of Delft (figure 5). The number of extracted lines varies with the parameter settings for the line growing algorithm. The settings used resulted in 397 lines with a minimum line length of 50 pixels. The standard deviation of the coordinates of the end points of the lines is modeled as follows:

$$\sigma = \frac{0.1}{\sqrt{l}} \ \text{mm} \qquad (\ 16 \ )$$

Where l is the line length in pixels. Then the largest standard deviation is 1.3 pixel. For the longest line (517 pixels) the standard deviation drops below 0.5 pixel. These values are chosen relatively high because of deformations present in this old building. Assuming a better precision, lines in some parts of the building would be excluded from their vanishing points.

Figure 5: Test image of a historic building in Delft

The result of the vanishing point detection is visualized in figure 3. In figure 4 on the left lines are shown that were not accepted as a member of one of the vanishing point clusters. Some lines obviously do not have a vanishing point orientation, for other lines – like the ones above and below the door – deformations of the building are suspected. The picture in the center of figure 4 shows lines that are adjusted for parallelism and perpendicularity constraints. In this example the maximum deviation from perpendicularity is 1.4 degree and the statistical test of the perpendicularity hypothesis was rejected. Lines that intersect with the first and third vanishing point (left and right in figure 3) are not adjusted because no choice for one of the vanishing points could be made. In figure 6 a part of the image is enlarged. The adjusted lines are shown in the upper half, the original lines extracted by line growing in the lower half of the figure. The angle between the adjusted lines and the original lines (1.2 degree) is due to deformations of the building in combination with the use of perpendicularity constraints. Without perpendicularity constraints the angle reduces to 0.7 degree.
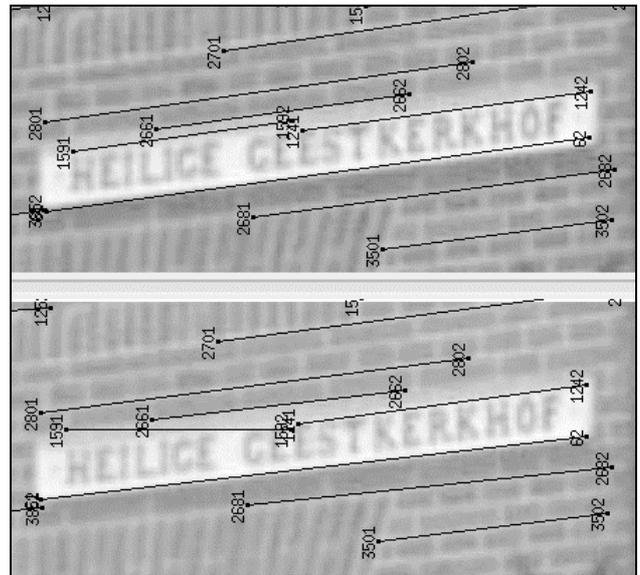

Figure 6: Enlargement showing adjusted (top) and original lines

In figure 4 on the right all the lines are pictured that are not adjusted. These are the lines that could not be (uniquely) grouped to one of the vanishing points. 30 of them are horizon lines. In table 1 results of clustering and statistical testing are summarised for both examples.

vanishing point	Example 1		Example 2	
	# lines (rejected)	$\frac{\hat{\sigma}^2}{\sigma_0^2}$	# lines (rejected)	$\frac{\hat{\sigma}^2}{\sigma_0^2}$
1	175 (1)	2.08	61(0)	0.32
2	130 (3)	1.67	160 (9)	1.26
3	104 (0)	1.25	20 (0)	2.49
all	349 (0)	1.49	202 (0)	1.05

Table 1: Results of the clustering and testing

4.2 Example 2: image of the faculty building

The second test image is an image of our faculty building (figure 7). Settings that were used for the line growing algorithm resulted in 250 lines with a minimum line length of 30 pixels. The standard deviation of the coordinates of the end points is a factor 2 smaller than in the previous example, but depends on the line length in the same way (equation 16). The largest standard deviation is close to 1 pixel. For the longest line (1062 pixels) the standard deviation drops to 0.17 pixel. The result of the vanishing point detection is visualized in figure 8. The order of the pictures is as in the previous example. From top left the first three images show the lines of the three vanishing points. The fourth image shows the lines that were not accepted as a member of one of the vanishing point clusters. It was concluded from visual inspection that non of these lines is expected to intersect at a vanishing point. Because the image is taken almost perpendicular to the façade, there are not many lines detected for the third vanishing point. In fact there is only one line of the third vanishing point visible (and detected) that has the spatial orientation of the third vanishing point (this is the line on top of the right tower of the building). The other 19 lines are all identified as horizon lines and thus excluded from the final adjustment (see bottom row of figure 8 with adjusted lines on the left and non-adjusted lines on the right). The adjustment only contains one perpendicularity condition between lines of the first and second vanishing point. The deviation from perpendicularity before adjustment was 0.065 degree and the statistical test of the perpendicularity hypothesis was accepted. Clustering and testing results are summarized in table 1.

Figure 7: Test image of the faculty building

5. CONCLUSIONS

A new method for vanishing point detection has been presented. This method is based on rigorous statistical testing and exploits the assumption of perpendicularity between the three major spatial orientations of the object lines. This assumption as well as the assumption of parallelism of object lines – the basic assumption for vanishing point detection – frequently holds for man-made objects like buildings.

The characteristics of the method can be summarized as follows:

- The method involves only a small number of parameters. Two types of parameters can be distinguished: parameters for the stochastic model of the observations and parameters for the statistical testing (i.e. the levels of significance).
- After detection of the first vanishing point the detection of second and third vanishing point is facilitated by the use of perpendicularity information. In the example of section 4.2 even a single line with the spatial orientation associated with the third vanishing point, was detected.
- The detection of lines on (or close to) the horizon line is part of the procedure.
- The adjusted spatial orientations of the lines that have been uniquely identified to intersect at a vanishing point, result as a by-product.
- The method is not designed for real-time applications because it is computationally expensive.

Although the new method has not been extensively tested and compared to existing techniques for vanishing point detection, the results of the presented tests show its suitability for architectural applications.

REFERENCES

Baarda, W., 1968. A testing procedure for use in geodetic networks. Netherlands Geodetic Commission, New Series, Vol. 2 (5), Delft.

Burns, J.B., A.R. Hanson, E.M. Riseman, 1986. Extracting straight lines. IEEE transactions on pattern analysis and machine intelligence, Vol. 8 (4), pp. 425-455.

Collins, R.T., 1993. Model Acquisition using Stochastic Projective Geometry. dissertation, Department of Computer Science, University of Massachusetts, Amherst.

Förstner, W., 1988. Model Based Detection and Location of Houses as Topographic Control Points in Digital Images. International Archives of Photogrammetry and Remote Sensing, Kyoto, Vol. 27 (B11-III), pp.505-517.

Heuvel, F.A. van den, 1997. Exterior Orientation using Coplanar Parallel Lines, 10th Scandinavian Conference on Image Analysis, Lappeenranta, pp. 71-78.

Heuvel, F.A. van den, and G. Vosselman, 1997. Efficient 3D-modeling of buildings using a priori geometric object information. Videometrics V, Sabry F. El-Hakim (ed.), SPIE Vol. 3174, pp. 38-49.

Lutton, E., H. Maitre and J. Lopez-Krahe, 1994. Contribution to the Determination of Vanishing Points Using Hough Transform. IEEE transactions on pattern analysis and machine intelligence, Vol. 16 (4), pp. 430-438.

Pla, F., J.M. Sanchiz, J.A. Marchant, R. Brivot, 1997. Building perspective models to guide a row crop navigation vehicle. Image & Vision Computing, Vol. 15 (6), pp. 465-473.

Shufelt, J.A., 1996. Performance Evaluation and Analysis of Vanishing Point Detection Techniques, ARPA Image

Understanding Workshop, Morgan Kaufmann Publishers, Palm Springs, pp. 1113-1132.

Straforini, M., C. Coelho and M. Campani, 1993. Extraction of vanishing points from images of indoor and outdoor scenes. Image and Vision Computing, Vol. 11 (2), pp. 91-99.

Williamson, J.R. and M.H. Brill, 1989. Dominant Geometry Combinations of Two- and Three-Point Perspective in Close-Range Applications. Photogrammetric Engineering and Remote Sensing, Vol. 55 (2), pp. 223-230.
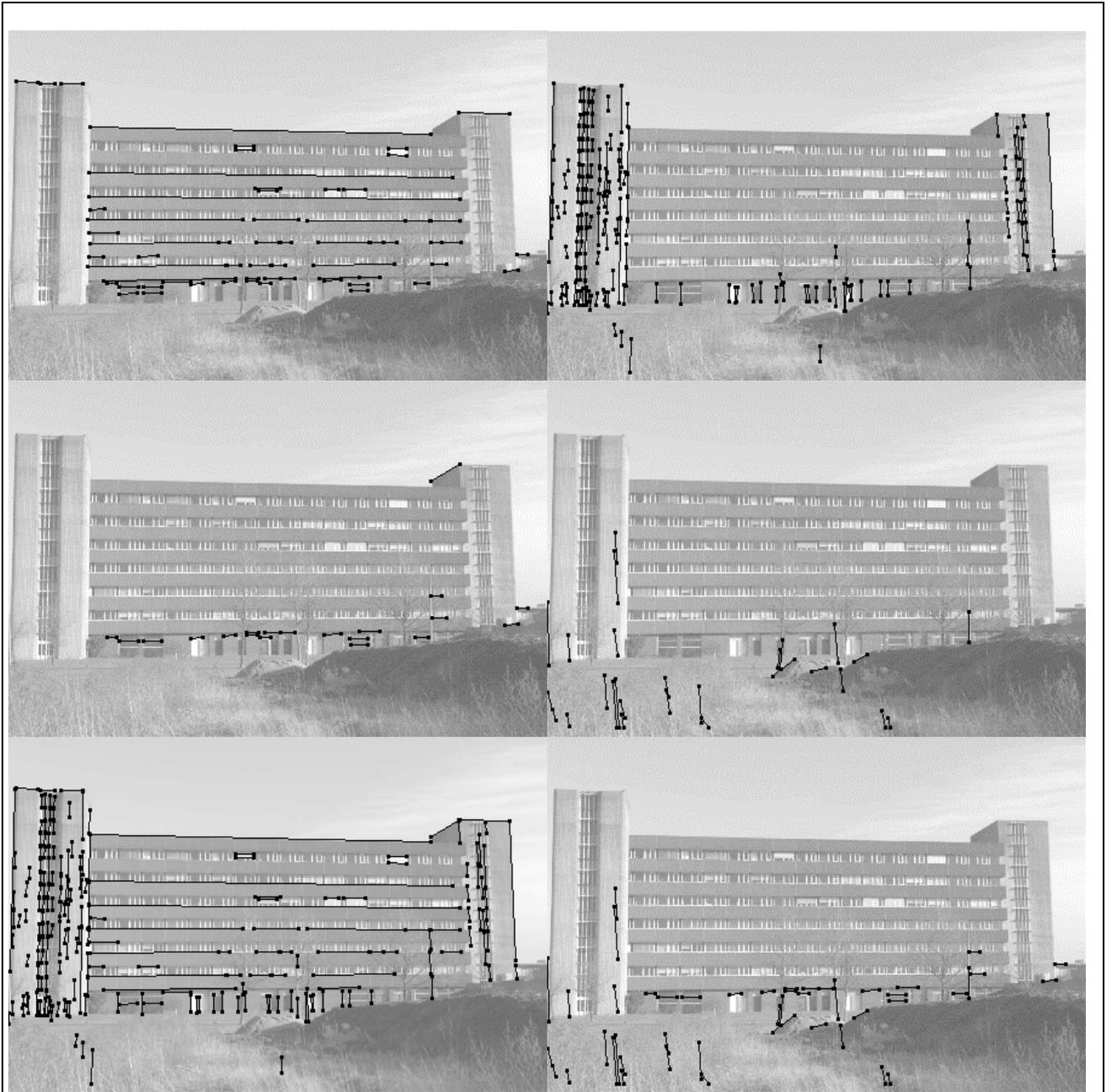
Figure 8: Vanishing point detection results for the image of the faculty building. From top left to bottom right: the lines of the three vanishing points, the rest of the lines, adjusted lines and non-adjusted lines